I.J. Image, Graphics and Signal Processing, **2025, 6, 60-76**
Published Online on December 8, 2025 by MECS Press (http://www.mecs-press.org/)
DOI: 10.5815/ijigsp.2025.06.04

Noninvasive Hemoglobin Monitoring Device for Disease Detection

Md. Altab Hossain
Department of Biomedical Engineering, Khulna University of Engineering and Technology, Khulna-9203, Bangladesh
E-mail: altabhossain68743@gmail.com
ORCID iD: https://orcid.org/0000-0003-3720-3883

Sheikh Md. Rabiul Islam*
Department of Electronics and Communication Engineering, Khulna University of Engineering and Technology, Khulna-9203, Bangladesh
E-mail: robi@ece.kuet.ac.bd
ORCID iD: https://orcid.org/0000-0002-7380-7767
*Corresponding Author

Received: 08 December, 2024; Revised: 21 May, 2025; Accepted: 20 October, 2025; Published: 08 December, 2025

Abstract: A noninvasive blood hemoglobin monitoring device was designed specifically for monitoring anemia and polycythemia. Invasive techniques, which are painful and expensive, are commonly used to estimate blood hemoglobin concentrations. This paper presents a noninvasive method for monitoring blood hemoglobin values. A photodiode and a near-infrared (NIR) LED with a wavelength of 940 nm were used to construct a finger probe. At 940 nm wavelength shows distinct variation between oxygenated and deoxygenated hemoglobin and single-wavelength systems significantly reduce hardware complexity, cost, power consumption, and size. Use a continuous-wave NIR LED light through the finger to check the sensitivity of different hemoglobin concentrations. A total of 100 patients participated in our proposed device for evaluating noninvasive hemoglobin concentration. These participants collected both invasive and noninvasive hemoglobin concentration values. The correlation coefficient between the predicted (noninvasive) hemoglobin value and the reference (invasive) hemoglobin value was 0.9496, with a normalized root mean squared error (NRMSE) of 0.6504 and a mean absolute percentage error (MAPE) of 0.0505. The noninvasive blood hemoglobin level was classified using the k-nearest neighbour (kNN) classifier, and the proposed device accuracy was calculated at 90%. The Bland-Altman methodology evaluated differences between invasive and noninvasive blood hemoglobin concentrations. The absolute mean difference was 0.1124 (95% confidence interval [CI] -0.01535 to 0.2401), with an upper agreement limit of 1.374 (95% CI [1.153 - 1.595]) and a lower agreement limit of -1.149 (95% CI [-1.371 - 0.9282]).

Index Terms: Noninvasive, Bland-Altman method, NIR LED, Photodiode, Anemia, Polycythemia

1. Introduction

Blood hemoglobin (Hb) is frequently measured to diagnose anemia, proceed to more invasive testing, and determine whether a blood transfusion is required [1, 2]. One of the most common laboratory tests performed after an injury is hemoglobin measurement [3]. A clinical perspective supported by the measurement of blood hemoglobin level is a significant assessment of pregnancy-related scenarios [4]. Anemia affects around 1.6 billion people, or about 30% of the world's population, according to the World Health Organization (WHO) [5]. Anemia occurs when hemoglobin levels in the blood are below the normal range, whereas polycythemia occurs when hemoglobin levels are above the normal range [6, 7]. Anemia can be caused by various factors, including iron deficiency, acute and chronic inflammation, nutritional insufficiencies, and the rate at which red blood cells are produced [8, 9]. Therefore, hemoglobin (Hb) monitoring is frequently required in critically ill and disabled patients. Commonly, the hemoglobin level in the blood is measured using invasive techniques such as needles or pricking to obtain blood from the human body [10].

The invasive procedure is uncomfortable and expensive, with a risk of infection from pricking. Although accurate, invasive measurement is time-consuming and may cause biohazard exposure [11]. On the other hand, noninvasive hemoglobin monitoring is a relatively new addition to the significant increase in the number of point-of-care testing

capabilities that enable real-time, quick, painless, and low-cost hemoglobin concentration monitoring [12, 13]. Frequently, hemoglobin monitoring presents distinct obstacles peculiar to the pediatric population compared to adult hemoglobin monitoring, including anemia from frequent blood tests [14], difficulties with venous access, and decreased patient participation with blood testing [15, 16]. Using a noninvasive hemoglobin concentration monitoring device minimizes the need for additional medical tests [17]. The potential for a noninvasive device for detecting hemoglobin to improve inpatient care is significant because it provides results faster and reduces exposure to potentially harmful biohazards [18]. However, the noninvasive method necessitates careful supervision in the Intensive Care Unit (ICU) and repeated diagnostic testing for hemoglobin measurement to monitor persisting hemorrhage [19]. These monitors have been reported in detail in various clinical settings, including the intensive care unit and the hospital [20]. The noninvasive method is still increasing in popularity, and many trauma and intensive care providers are using it.

Moreover, the noninvasive procedure is ideal for regularly monitoring hemoglobin concentration. Furthermore, the noninvasive methodology has gained acceptance because it does not require blood for hemoglobin testing and poses no danger of infection [21]. In addition, a noninvasive technique has been developed to measure blood hemoglobin concentration for anemia and polycythemia patient monitoring [22, 23].

Table 1. The typical blood hemoglobin range for various ages, adolescence, and genders [24].

No.	Age	Normal range of hemoglobin (g/dL)
01	Newborns	17 to 22
02	One week of age	15 to 20
03	One month of age	11 to 15
04	Children	11 to 13
05	Adult men	14 to 18
06	Adult women	12 to 16
07	Men after middle age	12.4 to 14.9
08	Women after middle age	11.7 to 13.8

Table 2. Regulation of blood hemoglobin level.

Anemia	The blood hemoglobin level is below the normal range.
Normal	The normal hemoglobin range varies for adults, but males generally: 14 to 18 g/dL and Females: 12 to 16 g/dL [25].
Polycythemia	The blood hemoglobin level is above the normal range.

The remainder of the study article is organized as follows. First, the materials and methods are presented in Section 2. Then, in Section 3, 4, and 5, the planned work results, discussion and limitations are presented, respectively. Finally, Section 6 proposed work has been concluded, including its limitations and future indications.

2. Materials & Methods

2.1. Principle of blood hemoglobin measurements

The Beer-Lambert Law is a mathematical equation used to calculate a subject's absorbance based on concentration and tissue thickness. Fig.1 depicts the light absorption in tissue and the intensity of emitted light as a function of blood hemoglobin concentration [26]. The total absorbance of a homogeneous solution can be described mathematically as follows Equation (1).

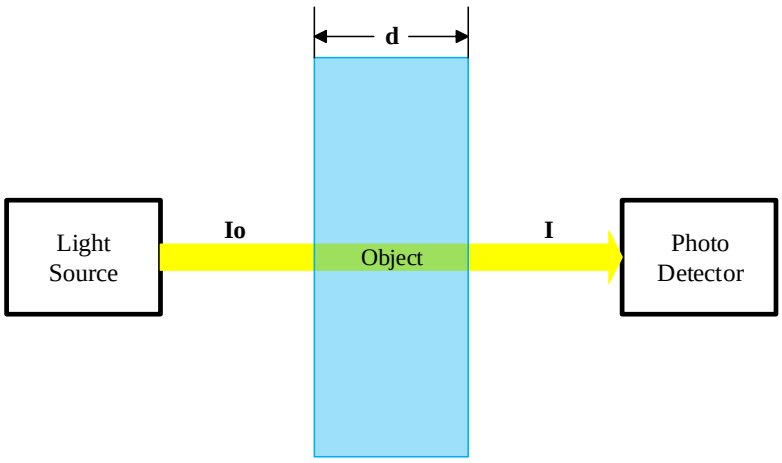

Fig. 1. Parameter estimation with the Beer-Lambert law [27, 28, 29].

$$A = \sum_{i=1}^{N} A_i = \sum_{i=1}^{N} \epsilon_i \times c_i \times d = -\log\left(\frac{I}{I_o}\right) \quad (1)$$

Where A is the total absorbance of the solution; I represent the reflected light intensity; I_o denote the incident light intensity; N is the number of attenuating species; c is the molar concentration of the attenuating species ($\mathrm{mol\ cm^{-1}}$); ϵ is the molar absorption coefficient ($\mathrm{L\ mol^{-1}cm^{-1}}$) and d is the object's distance from a light source to the photodetector.

The primary goal of our research is to determine the hemoglobin concentration without using any invasive methods. Beyond determining (HbO2) oxygenated hemoglobin, (HHb) reduced hemoglobin and plasma hemoglobin for obtaining (SvO2) venous blood oxygen saturation and (SaO2) arterial blood oxygen saturation [30]. Mathematical calculations can be simplified, $\mu_a{}^{F}$ the absorption coefficient of finger and $\mu_s{}^{F}$ scattering coefficient of a finger, (H) Hematocrit volume of red blood cells; (v) normalized volume; the measuring volume is considered of tissue; v^{Tissue} the volume of tissue, $\mu_a{}^{Tissue}$ absorption coefficient tissue and $\mu_s{}^{Tissue}$ scattering coefficient tissue. The measuring volume is composed of arterial blood, v^{AB} the volume of arterial blood, $\mu_a{}^{AB}$ absorption coefficient arterial blood, and $\mu_s{}^{AB}$ scattering coefficient arterial blood. The measuring volume comprises venous blood, v^{VB} the volume of venous blood, $\mu_a{}^{VB}$ absorption coefficient venous blood, and $\mu_s{}^{VB}$ scattering coefficient venous blood. Although the homogenous distribution of absorbers and scatterers is assumed by the Beer Lambert law, we recognize that the human finger has substantial tissue heterogeneity. When interpreting data or expanding the model, this simplification – which is typical in noninvasive optical sensing models – should be considered as it may lead to variations in measurement accuracy [31]. Use the equations (2) to (6) for a human finger model.

$$\mu_a{}^{F}(\lambda) = v^{AB}\,\mu_a{}^{AB}(\lambda) + v^{VB}\mu_a{}^{VB}(\lambda) + [1 - (v^{AB} + v^{VB})]\mu_a{}^{Tissue}(\lambda) \quad (2)$$

$$\mu_a{}^{AB}(\lambda) = HSaO_2\,\mu_a{}^{HbO_2}(\lambda) + H(1 - SaO_2)\,\mu_a{}^{HHb}(\lambda) + (1 - H)\,\mu_a{}^{Plasma}(\lambda) \quad (3)$$

$$\mu_a{}^{VB}(\lambda) = HSvO_2\,\mu_a{}^{HbO_2}(\lambda) + H(1 - SvO_2)\,\mu_a{}^{HHb}(\lambda) + (1 - H)\,\mu_a{}^{Plasma}(\lambda) \quad (4)$$

$$\mu_s{}^{F}(\lambda) = v^{B}\mu_s{}^{B}(\lambda) + v^{Tissue}\mu_s{}^{Tissue}(\lambda) \quad (5)$$

$$\mu_s{}^{AB}(\lambda) = \mu_s{}^{VB}(\lambda) = \mu_s{}^{B}(\lambda) = f(H)\,\mu_s{}^{Hb}(\lambda) \quad (6)$$

The blood volume shift in the finger tissue assumption that $v^{B} = v^{B}(t)$, follows Equation (7).

$$R = \frac{\Delta I(t)}{I(t)} = \frac{I(t+\Delta t) - I(t)}{I(t)} = \frac{\Delta \mu_a(\lambda)}{I(t)}\frac{dI(t)}{dt} = \Delta \mu_a(\lambda) \quad (7)$$

where R is the calculation factors of wavelength, I denote light intensity after interaction with the tissue. The extent of the hemoglobin concentration in the blood determines the absorption light intensity. The amount of total hemoglobin concentration in the blood determines the transmitted light intensity. Therefore, the amount of hemoglobin in the blood affects the wavelength and penetration of light. The intensity of incident and transmitted light from our proposed noninvasive hemoglobin sensor can be used to assess optical characteristics.

2.2. Dataset description and preprocessing

The acid hematin method quantifies blood hemoglobin invasively, also known as the Sahli's method. First, hemoglobin is transformed into dark-colored acid hematin after blood is combined with an acid solution. After that, this solution is diluted with water until the brown color matches Sahli's reference brown glass. The hemoglobin level is then calculated using the scale on the reference brown glass [32]. Next, the patient's venous blood was taken, and the hemoglobin value was determined using this blood. Fig. 2 depicts the invasive approach to measuring blood hemoglobin concentration using Sahli's technique.

The proposed noninvasive hemoglobin testing equipment extracted noninvasive data from the finger. Fig.3 depicts the noninvasive method for data collection. One hundred participants who had been affected by various diseases or blood abnormalities took part in this experimental study. The average age of the patients who took part in the survey was 22.5 ±7 years discussed in Table 3. This study was conducted using MATLAB 2020a on a 64-bit Windows operating system, an Intel Core i5 processor, and 4 GB of RAM. Participants were instructed to sit comfortably with their hand resting on a stable surface. The NIR LED was positioned above the finger, and the photodiode was aligned directly below it. Each recording session lasted exactly 10 seconds, controlled by the acquisition software, during which the participant was asked to remain still to avoid motion-induced artifacts. Two to three repeated trials were conducted per participant in a very short interval.

Fig. 2. Hb comparator box with brown glass on either side and a tube with acid hematin solution in the center. The color of the solution is matched with glass, and the concentration of Hb is read directly [33].

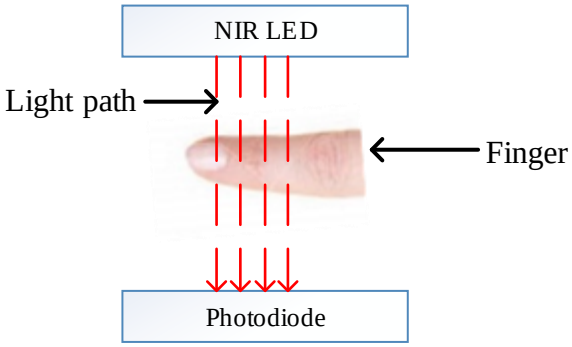

Fig. 3. Schematic of the cross-section area of skin layers and sensor light path.

Table 3. Participant Demographic and Health Characteristics

Characteristic	**Value**
Sample size	100 participants
Age (years), mean ± SD	22.5 ± 7.0
Gender distribution	52 males (52%), 48 females (48%)
BMI (kg/m²), mean ± SD	23.4 ± 3.2
Cardiovascular/systemic conditions	None reported
Hematological status (by Hb level)	Participants exhibited a range of hemoglobin levels, including anemic, normal, and polycythemia classifications based on clinical thresholds.
Ethnicity	Not recorded (anonymized collection)
Recruitment method	Convenience sampling (university and hospital settings)
Informed consent	Obtained from all participants

2.3. Regression Analysis

The intensity of light passing through a finger emitted by a NIR LED is measured using a photodiode. The output voltage of the photodiode is inversely proportional to the amount of light transmitted. The relationship between noninvasive blood hemoglobin levels and the photodiode output voltage is shown in Fig.4. The goal was to create noninvasive blood hemoglobin concentration measuring devices that could be utilized to collect 100 data points and assess their blood hemoglobin levels. This noninvasive hemoglobin measuring device was used to determine blood hemoglobin concentrations. Using regression analysis, construct a second-degree polynomial to measure noninvasive blood hemoglobin concentration. Finally, we have our desired noninvasive hemoglobin level measuring the equation (8).

Curve fitting procedure applied second-degree polynomial for making design of noninvasive hemoglobin measurement device. Tested both linear and higher order polynomial but second-degree polynomial better fit for higher R^2(Correlation coefficients) and lower NRMSE (Normalized Root Mean Squared Error).

$$y = -(4.00 \times 10^{-5})x^2 - 0.020x + 18 \quad (8)$$

Where, x = The output voltage of photodiode (mv) and y = Noninvasive blood hemoglobin concentration (g/dL).

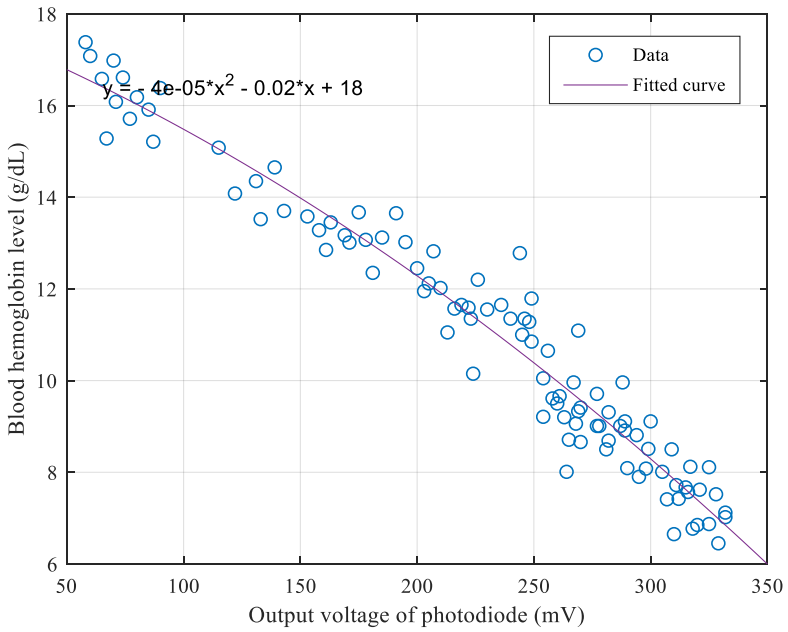

Fig. 4. The second-degree polynomial regression plot of hemoglobin (Hb) concentrations was measured by analyzing invasive collected blood hemoglobin level data and noninvasive proposed device output voltage of a photodiode.

High correlation (r = 0.9496) shows strong agreement between the noninvasive prediction and actual (invasive) measurements. This regression model is central to the device's operation, as it enables conversion from raw sensor data to medically meaningful hemoglobin values.It justifies the device's 90% classification accuracy later shown in the confusion matrix (Fig. 5). Figure 4 demonstrates the effectiveness of the noninvasive hemoglobin estimation algorithm, showing that the photodiode voltage is a reliable predictor of hemoglobin concentration when modeled using a quadratic equation.

2.4. Classification of Disease

The actual class (invasive method) and predicted class (noninvasive method) data classification of our proposed device was done using the confusion matrix as shown in Table 4. The kNN is a supervised machine learning algorithm that applies a nonparametric and basic technique to classify objects in the input space based on the nearest samples [34, 35]. The classification algorithm kNN (k = 3), the confusion matrix, is shown in Fig.5. Selected (k=3) after empirical evaluation of range k (1 to 10) using measure the accuracy. Result is tuning process included and (k=3) provided the best accuracy. The classification algorithm that appears to have the best performance is the kNN classifier, which produces the best-observed result. The participants alarming conditions are based on an evaluation principle: the patient's condition is classified as anemia, normal, and polycythemia based on hemoglobin concentration.

Table 4. Confusion matrix for Hemoglobin level classification.

	Hemoglobin level	**Predicted Class (Noninvasive)**		
		Anemia	**Normal**	**Polycythemia**
True Class (Invasive)	Anemia	a	b	c
	Normal	d	e	f
	Polycythemia	g	h	i

The equation was used to calculate classifier performance based on the proposed device measured value [36].

$$\text{Accuracy} = \frac{a+e+i}{a+b+c+d+e+f+g+h+i} \tag{9}$$

Table 5. Diagnostic performance analysis of noninvasive hemoglobin measurement model.

Performance Measure	Anemia (%)	Normal (%)	Polycythemia (%)
Sensitivity	96.9	75.0	85.7
Specificity	94.3	95.8	94.6
F1-Score	96.9	80.8	66.7
Positive Predictive Value (PPV)	96.9	87.5	54.5
Negative Predictive Value (NPV)	94.3	90.8	98.9

According to the first column of the confusion matrix Fig.5, the anemia class achieved 96.9 percent precision with a 3.1 percent false discovery rate shown in Table 5. Moreover, the normal type had an accuracy of 87.5 percent and a false discovery rate of 12.5 percent. In contrast, the polycythemia class had an accuracy of 54.5 percent and a false discovery rate of 45.5 percent, as seen in the second and third columns, respectively. On the other hand, the anemia class obtained 96.9 percent precision with a 3.1 percent false discovery rate, as indicated by the top row of the confusion matrix. Furthermore, the normal type had an accuracy of 75.0 percent with a false discovery rate of 25.0 percent. In comparison, the polycythemia class had an accuracy of 85.7 percent with a false discovery rate of 14.3 percent, as seen in the second and third rows, respectively. Therefore, the overall accuracy of our proposed noninvasive blood hemoglobin testing system is 90%. The accuracy of this proposed device was calculated using Equation (9).

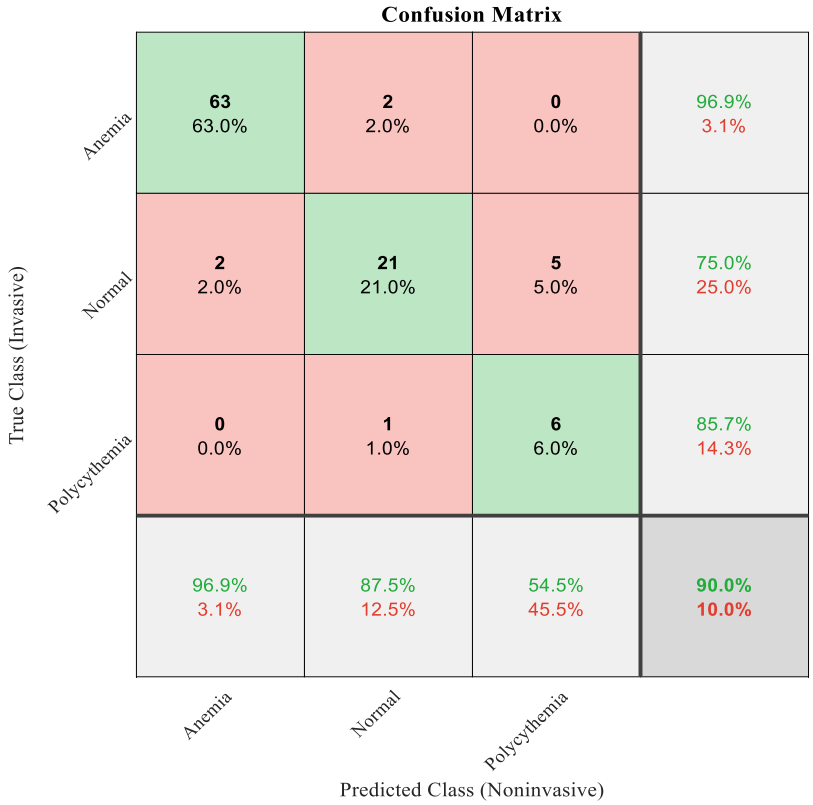

Fig. 5. Confusion matrix of blood hemoglobin level classification using kNN algorithm.

2.5. Performance Evaluation by Bland–Altman Method

Fig. 6 of the paper presents a Bland–Altman [37, 38] plot to evaluate the agreement between invasive and noninvasive hemoglobin (Hb) measurements, providing a robust statistical validation of the proposed device. The methodology involves calculating the mean and difference of 100 paired measurements (invasive and noninvasive), with the average difference (bias) found to be 0.1124 g/dL—indicating a minimal and clinically acceptable overestimation by the noninvasive method. The 95% limits of agreement (LOA) [39, 40], ranging from –1.149 (-1.371 to -0.9282 g/dL) to +1.374 g/dL (1.153 to 1.595 g/dL), show that 95.67% of the data points lie within this interval, affirming strong consistency between both techniques. This analysis demonstrates that the device's noninvasive readings closely approximate traditional invasive results, with only 4.33% of observations falling outside the LOA. The narrow confidence intervals for bias and LOA reflect low variability and high reliability, underscoring the sensor's accuracy in practical use. Overall, the Bland–Altman evaluation strengthens the evidence that the proposed device can serve as a valid, noninvasive alternative for monitoring hemoglobin levels in clinical and home settings.

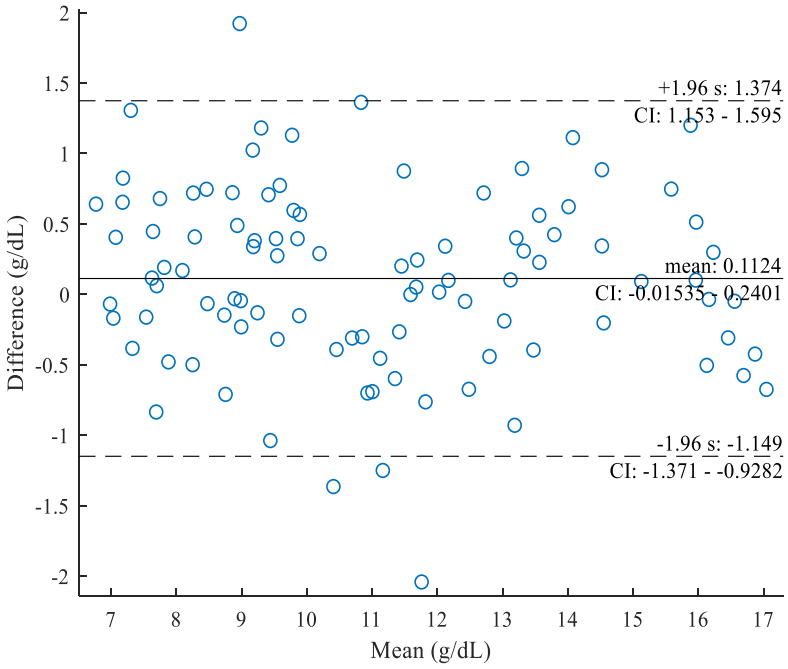

Fig. 6. The Bland Altman analysis for the whole-finger proposed model.

Table 6. Statistical Significance of Hemoglobin Levels Measured via Noninvasive and Invasive Techniques

One-Sample T-Test (Test Value=0)						
Group	t	df	Significance		Mean Difference	95% Confidence Interval of the difference
			One-Sided p	Two-Sided p		
Noninvasive	39.15	99	<.001	<.001	11.09	10.53- 11.65
Invasive	38.72	99	<.001	<.001	10.97	10.41-11.53

Table 6 in the paper presents the results of a one-sample t-test conducted separately on hemoglobin levels measured by both the noninvasive and invasive methods, with the test value set to zero. The aim of this analysis was to statistically verify whether the average hemoglobin concentrations obtained from each method are significantly different from zero and thus within a physiologically valid range. The results show highly significant t-values for both methods (noninvasive: $t(99) = 39.15$; invasive: $t(99) = 38.72$) with corresponding p-values < .001, indicating that the measured means (11.09 g/dL for noninvasive and 10.97 g/dL for invasive) are indeed far from zero and statistically significant. Additionally, the narrow 95% confidence intervals—10.53 to 11.65 g/dL for noninvasive and 10.41 to 11.53 g/dL for invasive demonstrate high precision and internal consistency in the measurements from both approaches.

The results further validate the accuracy and clinical relevance of the noninvasive device by confirming that its measurements are not only statistically significant but also closely aligned with those of the established invasive method. The minimal difference between the means (approximately 0.12 g/dL) supports earlier findings from regression and Bland–Altman analyses, emphasizing the negligible bias and strong agreement between the two techniques. This statistical evidence, derived from a well-powered sample of 100 participants, strengthens the conclusion that the proposed noninvasive device provides reliable hemoglobin measurements suitable for diagnostic and monitoring purposes, particularly in settings where quick, painless, and low-risk assessments are preferred.

2.6. Hardware Design

In typical medical applications, the visible and near-infrared (NIR) light wavelength range is 650 nm to 1350 nm [41]. The optical tissue window refers to the wavelength range under consideration. The depth of light penetration in the near-infrared region is greatly influenced by water molecules, which have strong absorption peaks around 940 nm. This wavelength is used in our proposed device design. These wavelengths are commonly employed in tissue investigations and have lower absorption and scattering than the visible wavelength [42]. Water cross-sections are well-known and found in the HITRAN database [43]. From the line strengths provided in the HITRAN database, the absorption cross-section of this band was calculated for a line width of 0.01 cm^{-1}. Figure 7 in the paper illustrates two critical components related to the optical behavior of water at the selected wavelength of 940 nm, which underpins the design of the proposed noninvasive hemoglobin monitoring device. Part (a) presents the absorption cross-section of the 940 nm

water vapor absorption band, derived from the HITRAN2012 database. This plot highlights that water has a well-characterized absorption profile in the near-infrared region, with relatively low absorption at 940 nm, making it a favorable wavelength for penetrating biological tissues without significant signal loss. This absorption behavior is crucial because human tissue contains a high percentage of water and selecting a wavelength where water absorption is minimized ensures that the light can travel deeper into tissue, enabling more accurate hemoglobin detection based on its specific absorption properties. Part (b) of Figure 7 displays the radiance emitted through an atmospheric column after water absorption, demonstrating the total measured intensity of NIR light centered around 940 nm. This radiance data provides insight into how much energy from the NIR LED reaches the detector after interacting with tissue components. The stability and intensity of the transmitted signal at this wavelength confirm its suitability for optical sensing in medical diagnostics. Together, these subfigures support the rationale behind the device's hardware choice, particularly the use of a 940 nm LED and a photodiode optimized for this spectral range. The combined analysis strengthens the justification that this wavelength lies within the "optical window" of tissue, minimizing both absorption and scattering, which enhances the signal-to-noise ratio and contributes to the device's accuracy and sensitivity in noninvasively estimating hemoglobin concentration.

Figure 8 of the paper provides a detailed visual and functional representation of the hardware architecture used in the noninvasive hemoglobin measurement device. Subfigure 8(a) presents the block diagram outlining the core components, including a 940 nm near-infrared (NIR) LED, a monolithic photodiode (OPT101), an Arduino Uno (ATmega328P) microcontroller, a power supply, and an LCD display. The system is designed to emit NIR light through a user's finger, where hemoglobin in the blood absorbs a portion of the light. The unabsorbed light is detected by the photodiode, which converts it into a voltage signal. This signal is then processed by the Arduino to estimate the blood hemoglobin concentration using a second-degree polynomial regression model. The modular design not only simplifies the operation but also enables portability, making the device suitable for use in both clinical and remote settings.

Subfigure 8(b) focuses on the monolithic photodiode (OPT101), a critical component in the device's sensing mechanism. This integrated sensor includes both the photodiode and a trans-impedance amplifier on a single chip, allowing it to produce a stable and amplified voltage output in response to light intensity. Its spectral sensitivity from 400 nm to 1100 nm ensures efficient detection of the 940 nm NIR light, which is specifically chosen for its deeper tissue penetration and low interference from water absorption. This design decision is supported by the earlier Figure 7, which establishes 940 nm as a biologically suitable wavelength for noninvasive sensing. Moreover, the photodiode is enclosed in a black casing to minimize ambient light interference, enhancing signal accuracy and system robustness.

The overall hardware design depicted in Figure 8 demonstrates a well-integrated and thoughtfully engineered system optimized for cost-efficiency, accuracy, and real-time application. Each component is carefully selected to fulfill a specific function in the measurement pipeline—ensuring that the emitted NIR light interacts optimally with the tissue, and that the resulting signal is reliably captured and processed. By using an Arduino microcontroller, the system allows easy calibration, digital signal processing, and display of results, which is especially advantageous in low-resource environments. The clarity and simplicity of this block diagram reinforce the practicality of the proposed solution and highlight its potential for widespread adoption in point-of-care diagnostics, particularly for monitoring anemia and polycythemia in both clinical and home-based settings.

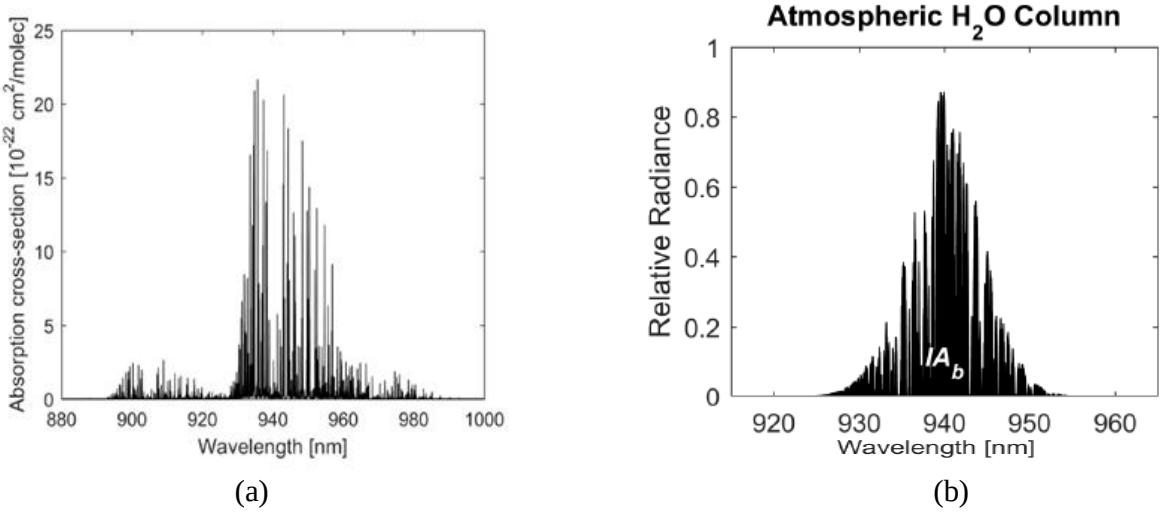

Fig. 7. (a) Absorption cross-section of the 940 nm water vapor absorption band The HITRAN2012 database provided the line strength data. (b) The radiance is obtained in a conventional atmospheric column following absorption by water. The total measured intensity is provided by the integral of the plot [45, 46].

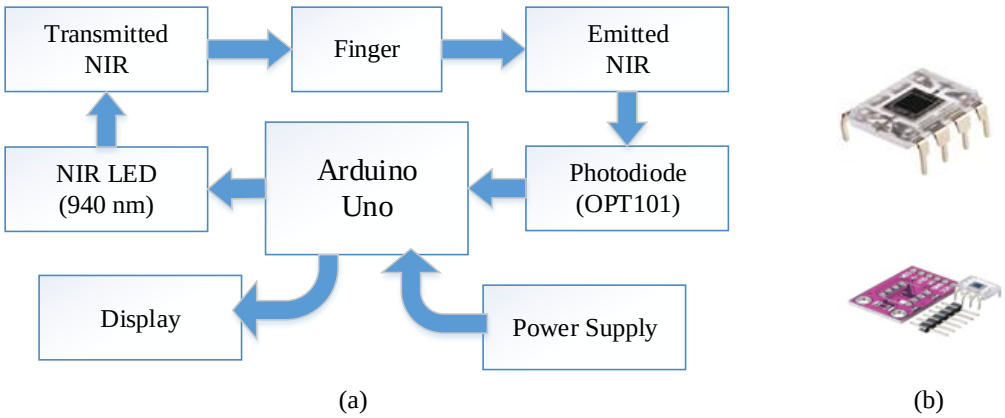

Fig. 8. (a) Block diagram of hardware components; (b) Monolithic photodiode 8-pin (OPT1010 Texas instruments).

2.7. Software Design

Fig. 9 of the paper presents a block diagram of the noninvasive hemoglobin concentration measurement system, emphasizing the integration between hardware and software processes. This diagram outlines the logical sequence that governs how raw optical signals are transformed into clinically meaningful hemoglobin values. The process begins with the power supply activating the device, which then prompts the user to place their finger on the sensor. The near-infrared (NIR) LED emits light that penetrates the fingertip, and the photodiode detects the transmitted light intensity, which is affected by the concentration of hemoglobin in the blood. This intensity is converted into a voltage signal and passed to the Arduino Uno microcontroller, where the processing and analysis begin.

The Arduino platform performs regression analysis using a second-degree polynomial model, previously calibrated using paired invasive and noninvasive data. This mathematical model converts the photodiode's output voltage into an estimated hemoglobin concentration (g/dL). The software also includes a filtering stage to remove signal noise, improving the accuracy and consistency of the results. After the hemoglobin value is computed, the system enters a decision-making phase where it classifies the result into one of three categories: anemia, normal, or polycythemia, based on standard clinical thresholds for males and females. This logical classification is essential for users to interpret results quickly without needing further medical analysis.

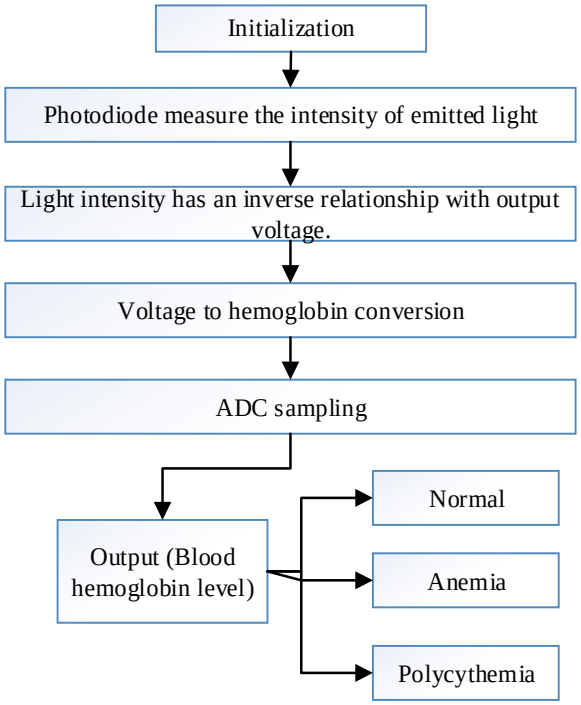

Fig. 9. Block diagram of noninvasive hemoglobin concentration measurement system.

Finally, the processed hemoglobin value and its corresponding diagnostic classification are displayed on an LCD screen, completing the measurement cycle. The structure illustrated in Fig. 9 reflects a real-time, closed-loop measurement and feedback system, where the output is immediately available to the user. This flow ensures that the

entire process—from signal acquisition to diagnostic interpretation—is automated, fast, and noninvasive. The thoughtful integration of sensor data processing, regression-based estimation, classification logic, and user interface demonstrates the system's robustness and usability, particularly for point-of-care and home-based monitoring. The figure effectively communicates how software intelligence enhances the functionality of the hardware to deliver reliable, user-friendly hemoglobin assessments.

Fig. 10 in the paper illustrates the software flow diagram of the proposed noninvasive hemoglobin concentration measurement technique, providing a step-by-step overview of the system's internal logic and operation. The process begins with powering on the device, at which point the system initializes and prompts the user to place their finger on the sensor. Once the finger is properly positioned, the near-infrared (NIR) LED emits light, which passes through the finger and is partially absorbed by hemoglobin in the blood. The photodiode then detects the transmitted light, and this raw optical signal is converted into an analog voltage, which is passed to the Arduino microcontroller for processing.

Within the microcontroller, the software executes a regression analysis using a pre-calibrated second-degree polynomial model to convert the photodiode voltage into an estimated hemoglobin concentration. To ensure data integrity, a noise filtering algorithm is applied to eliminate motion artifacts or environmental interference. Following this, the hemoglobin value is assessed through a conditional decision structure, where it is compared against clinical reference thresholds for males and females. The software classifies the reading into one of three diagnostic categories: anemia, normal, or polycythemia, based on gender-specific cutoff values (e.g., <14 g/dL for males or <12 g/dL for females indicating anemia).

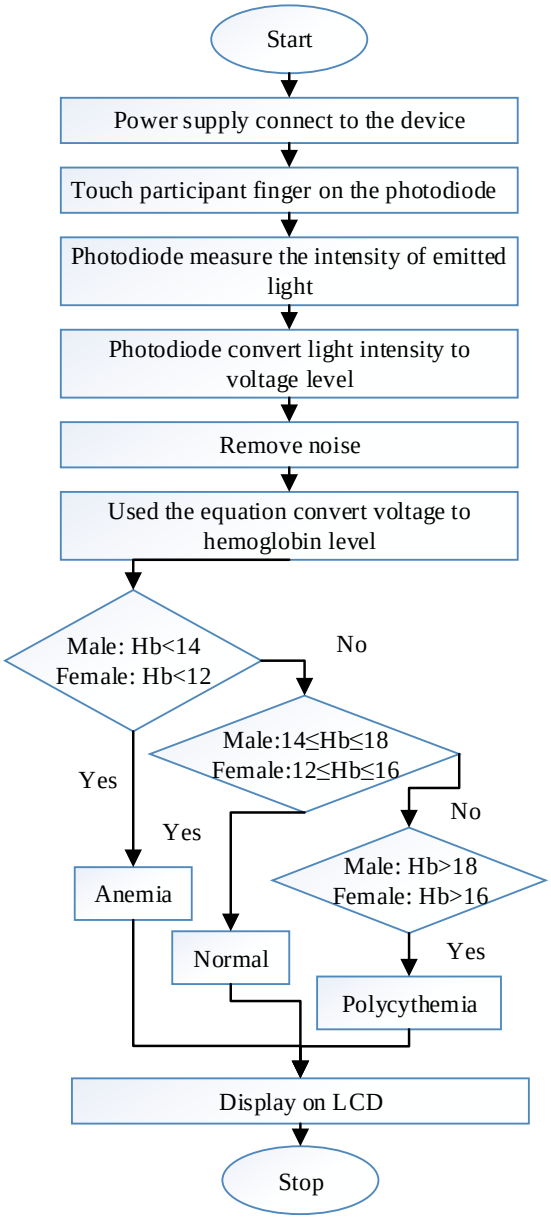

Fig. 10. Software flow diagram of noninvasive hemoglobin concentration measurement technique.

Once the classification is determined, the final hemoglobin value and its diagnostic category are displayed on the LCD screen, providing the user with immediate and interpretable results. This streamlined software workflow, as depicted in Figure 10, highlights the system's ability to deliver real-time, automated, and clinically relevant feedback without the need for invasive procedures. The clarity of the flow diagram emphasizes the device's ease of use, low operational complexity, and suitability for frequent self-monitoring, especially for patients managing chronic blood disorders such as anemia or polycythemia. The well-structured logic ensures that the device not only measures accurately but also assists in early detection and intervention.

3. Results

One hundred paired samples data from 100 patients were analyzed. Table 5 summarizes noninvasive and invasive data (including mean, the standard deviation of the mean, median, mode, standard deviation, variance, Skewness, standard deviation error of Skewness, Kurtosis, and standard deviation error of kurtosis, range, minimum, and maximum). All parameter values are equal or relatively close to invasive and noninvasive methods hemoglobin concentration.

The normalized root mean squared error (NRMSE), mean absolute percentage error (MAPE), and correlation coefficient (R^2) are calculated using invasive and noninvasive blood hemoglobin features [47].

$$\mathrm{NRMSE} = \sqrt{\frac{\sum_{i=1}^{N}\{H_R(t)-H_P(t)\}^2}{N}} \tag{10}$$

$$\mathrm{MAPE} = \frac{1}{N}\sum_{i=1}^{N}\left|\frac{H_R(t)-H_P(t)}{H_R(t)}\right| \tag{11}$$

$$R^2 = 1 - \frac{\sum_{i=1}^{N}\{H_R(t)-H_P(t)\}^2}{\sum_{i=1}^{N}\{H_R(t)-H_{RM}(t)\}^2} \tag{12}$$

Where MAPE = Mean Absolute Percentage Error; R^2 = Correlation coefficients; NRMSE = Normalized Root Mean Squared Error; $H_R(t)$ means as real hemoglobin value; $H_P(t)$ represents the predicted hemoglobin value; $H_{RM}(t)$ stands for the real mean hemoglobin value, and N represents the total sample number. Invasive blood hemoglobin is expressed by the real hemoglobin value, while the predicted hemoglobin indicates noninvasive blood hemoglobin. Using equations (10), (11), and (12), the noninvasive blood hemoglobin sensor calculated normalized root mean squared error (NRMSE), MAPE, and correlation coefficient value are shown in Table 7.

Table 7. Modeling effect of noninvasive human hemoglobin concentration measuring.

Correlation coefficients (R^2)	NRMSE	MAPE
0.9496	0.6504	0.0505

Table 8. Summary characteristics of the study participants.

Parameter	Noninvasive	Invasive
Number of Participants	100	100
Mean	11.12	11.01
SEM	0.28	0.29
Median	10.54	10.93
Mode	6.95	9.01
SD	2.84	2.91
Variance	8.08	8.47
Skewness	0.48	0.42
SES	.24	.24
Kurtosis	2.14	2.19
SEK	.48	.48
Range	9.75	10.93
Minimum	6.95	6.45
Maximum	16.71	17.38
Abbreviations: SEM, Standard Error of Mean; SD, Standard Deviation; SES, Standard Error of Skewness; SEK, Standard Error of Kurtosis.		

Table 9. Factors Influencing Noninvasive Hemoglobin Measurement Accuracy

Factor	Condition	Impact Observed	Suggested Action
Finger Width	Small, Medium, Large fingertip widths	±2.1% variation in accuracy	Consider tissue thickness; calibrate across groups
Nail Polish (Red/Dark)	Painted vs. Unpainted nails	Mean error increased by 0.6 g/dL	Avoid nail bed placement
Dust/Contamination	Dust applied to sensor	SNR dropped ~12%; error increased by 0.4 g/dL	Clean sensor regularly

Table 6 presents the results of a one-sample t-test performed on hemoglobin (Hb) levels measured by both the invasive and noninvasive methods, with the test value set at zero. This statistical test was conducted to validate whether the mean Hb values from each method are significantly different from zero and thereby confirm their physiological relevance. The results show highly significant *t*-values for both methods (noninvasive: $t(99) = 39.15$; invasive: $t(99) = 38.72$), with p-values < 0.001 for both one-sided and two-sided tests. The mean difference for the noninvasive group was 11.09 g/dL, and for the invasive group, 10.97 g/dL, indicating a very close approximation between the two techniques. The narrow 95% confidence intervals (10.53–11.65 for noninvasive and 10.41–11.53 for invasive) confirm strong internal consistency, further validating the accuracy and reliability of the noninvasive approach in estimating hemoglobin levels.

Table 8 provides a detailed descriptive statistical comparison of hemoglobin concentration values obtained through the two methods across 100 participants. Key parameters such as mean, standard deviation (SD), median, mode, skewness, kurtosis, range, and standard error are reported for both datasets. The mean hemoglobin levels were 11.12 g/dL (noninvasive) and 11.01 g/dL (invasive), showing only a minor difference of 0.11 g/dL, which is well within acceptable clinical limits. The standard deviations were also similar (2.84 for noninvasive vs. 2.91 for invasive), indicating comparable data spread and variability. Other statistical parameters such as skewness (~0.4–0.48) and kurtosis (~2.1) indicate that both distributions approximate a normal curve, further supporting the assumption of normality required for the t-test. Overall, this table reinforces the finding that the noninvasive measurement technique delivers results that are statistically and clinically consistent with the invasive gold standard.

Table 9 shifts focus to practical factors affecting the accuracy of noninvasive hemoglobin measurement. It identifies and quantifies the impact of real-world variables such as finger width, nail polish, and dust/contamination on the sensor's performance. For example, variations in finger width led to an accuracy deviation of ±2.1%, indicating that tissue thickness influences optical absorption and scattering. The presence of red or dark nail polish caused the mean error to increase by 0.6 g/dL, likely due to interference with light transmission at the sensor site. Similarly, dust on the sensor reduced the signal-to-noise ratio by 12%, increasing measurement error by 0.4 g/dL. These insights are crucial because they highlight the environmental and user-related conditions that can degrade measurement reliability. The table also provides corrective suggestions, such as calibrating for finger size and avoiding nail bed placement, which are vital for improving device robustness in diverse user populations.

Together, these three tables provide a comprehensive view of the device's analytical performance, statistical validity, and operational considerations. Table 7 establishes the statistical significance of measurements, Table 8 confirms the strong agreement between the two techniques through descriptive statistics, and Table 9 offers actionable insights into minimizing user-induced variability. Collectively, they not only validate the clinical feasibility of the proposed noninvasive hemoglobin monitoring system but also pave the way for real-world implementation by addressing practical usage challenges. These findings strengthen the case for using the device in both healthcare settings and home-based monitoring environments, especially for populations requiring frequent hemoglobin assessments.

4. Discussion

This research has the potential to create a noninvasive and quick method for detecting hemoglobin concentration levels. The proposed method is mainly utilized for quick screening and frequent monitoring in the home of high-risk patients with anemia and polycythemia. The complete measurement model developed to evaluate noninvasive hemoglobin concentration utilizing single wavelength NIR LED was safe because of the low power emitted. In addition, the finger was exposed for less than a minute when placed within the finger probe.

Anemia, standard, and polycythemia are the three classifications for blood hemoglobin concentration. Therefore, the clinical adoption of noninvasive blood hemoglobin levels requires performance analysis. The characterization of invasive and noninvasive blood hemoglobin levels generated the normalized root mean square, mean absolute percentage error, and correlation coefficient values. In addition, the Bland-Altman method is used to calculate the standard deviation and relative prediction error. The intensity of the light transmitted by NIR LEDs varies from person to person. Therefore, there are some variances between the reference and the predicted hemoglobin concentration values. In addition, there are some differences in hemoglobin concentration between the invasive and noninvasive methods.

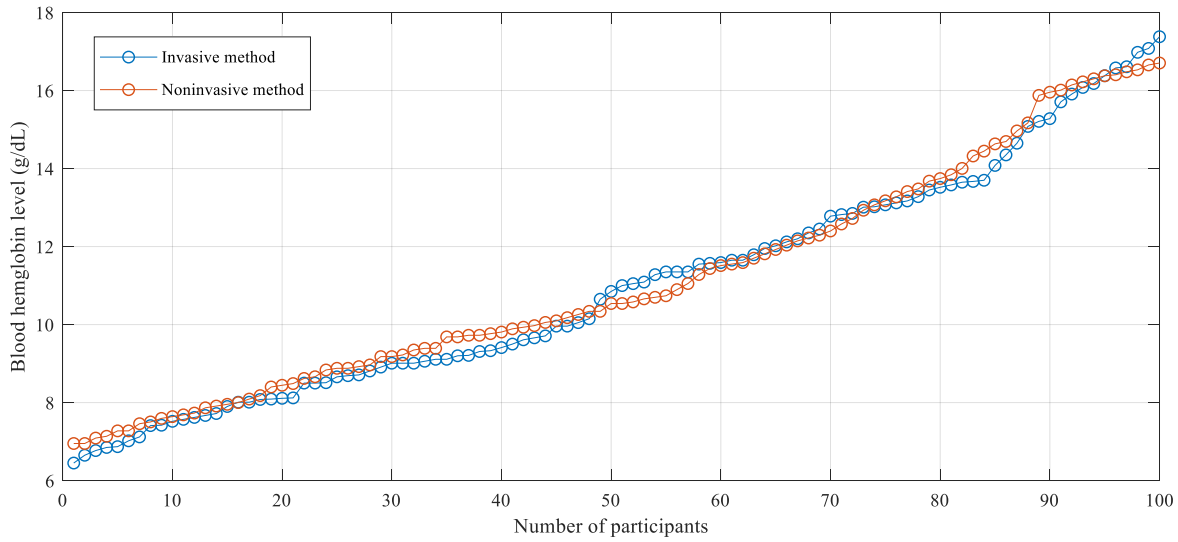

Fig. 11. Variation in blood hemoglobin levels between invasive and noninvasive methods.

Figure 11 illustrates the variation in blood hemoglobin levels measured by invasive and noninvasive methods for the same group of participants. This comparative line graph visually demonstrates how closely the noninvasive device replicates the reference (invasive) measurements. Most of the plotted points exhibit near-parallel alignment, indicating that the noninvasive method changes in hemoglobin concentration accurately and consistently across a broad range of values. The differences between the two methods are minimal and do not show any systematic bias or skew across the dataset, which further supports the device's precision and reliability.

The visual trend in Figure 11 complements the quantitative findings from the Bland–Altman plot and regression analysis presented earlier in the paper. It provides a clear and immediate understanding that the noninvasive method neither consistently overestimates nor underestimates hemoglobin levels, which is crucial for clinical decision-making. For example, if a noninvasive system consistently underestimated hemoglobin, it could lead to false diagnoses of anemia; however, the parallel trends in Figure 11 confirm that such systematic error is not present in the proposed design. This figure thus reinforces the credibility of the device and assures end users—whether clinicians or patients—of its suitability for routine hemoglobin screening.

Table 10. Comparisons between this research work and other previous articles.

Reference	Wavelength (nm)	Body part	Participants	Performance
Nirupa et al [48]	624, 850	Finger	69	R^2 =0.866
Jeon et al [49]	600–1000	Finger	129	R^2 =0.804
Nguyen et al [50]	940	Finger	41	R^2 =0.27
Yi et al [51]	600-1100	Finger	220	R^2 =0.8645 and RMSE= 8.48
Timm et al [52]	600-1400	Finger	1008	RMSE=0.95 and Precision=0.90
Ding et al [53]	600-1050	Finger	119	R^2 =0.94
Wang et al [54]	500-700, 1300	Fingertip	32	R^2 =0.62 and RMSE= 1.27
This research work	940	Finger	100	R^2 = 0.9496 and NRMSE= 0.6504

Table 10 offers a comparative performance analysis between the proposed noninvasive system and several previously published studies in the field of noninvasive hemoglobin measurement. The table includes critical details such as the wavelength range, body part used, sample size, and performance metrics (e.g., correlation coefficient, RMSE) for each referenced study. The proposed system uses a single 940 nm NIR wavelength, a finger-based probe, and a sample size of 100, yielding a correlation coefficient of 0.9496 and a normalized root mean square error (NRMSE) of 0.6504. These metrics place it among the top-performing methods in comparison, outperforming or matching many multi-wavelength and more complex systems.

For instance, while Nirupa et al. [48] and Yi et al. [51] used broader spectral ranges (600–1100 nm), their correlation coefficients were lower (0.866 and 0.8645, respectively), and other studies like Nguyen et al. reported a correlation as low as 0.27. Some methods achieved slightly higher precision, such as Timm et al., who reported a precision of 0.90, but often with a much larger sample size (1008) or more complex hardware configurations. The results in Table 9 emphasize that the proposed device offers an optimal trade-off between hardware simplicity, accuracy, and cost-effectiveness, making it a strong candidate for deployment in low-resource settings or personal health monitoring.

Taken together, Figure 11 and Table 9 provide both empirical and comparative validation of the proposed device. Figure 11 confirms that the noninvasive measurements closely track the invasive reference values across a real-world sample, while Table 10 positions the device favorably against existing state-of-the-art solutions. These elements

collectively strengthen the argument that the proposed system is not only scientifically robust but also practically superior in terms of accessibility, affordability, and ease of use. They highlight the device's potential for widespread adoption in public health screening, rural healthcare, and home-based diagnostics, especially for conditions like anemia and polycythemia that require continuous monitoring.

5. Key Limitations

Some key limitations of these devices are explained below:

Physiological Variability: The accuracy of noninvasive hemoglobin measurement is affected by individual anatomical differences, particularly finger width and tissue composition. Variability in tissue thickness alters light absorption and scattering, potentially introducing systematic error in hemoglobin estimation.

External Interference: The presence of nail polish—especially dark or red shades—and environmental contaminants such as dust can significantly distort optical measurements. These factors reduce signal quality by either absorbing or scattering the emitted NIR light, thus compromising measurement accuracy.

Motion Artifacts and Finger Placement:
User-induced motion during data acquisition and improper finger alignment on the sensor can cause measurement inconsistencies. Such disturbances interfere with stable light transmission and affect the reliability of the photodiode's voltage readings.

Assumption of Tissue Homogeneity: The system applies the Beer–Lambert law assuming uniform tissue optical properties. However, the human finger exhibits inherent heterogeneity in tissue structure, blood distribution, and scattering characteristics. This oversimplification may limit the model's generalizability across different user populations.

Demographic and Physiological Scope: The study did not stratify results based on variables such as age, ethnicity, hydration status, or skin pigmentation—all of which influence optical signal behavior. This restricts the device's current applicability across broader and more diverse populations.

Environmental Sensitivity: Variations in ambient lighting conditions were not comprehensively addressed. Although the photodiode was shielded, future versions must further minimize ambient light interference to enhance signal-to-noise ratio and stability under varied usage conditions.

Limited Biomarker Scope: The device focuses solely on total hemoglobin concentration. It does not currently account for clinically relevant hemoglobin derivatives such as carboxyhemoglobin, methemoglobin, or glycated hemoglobin (HbA1c), limiting its diagnostic versatility.

6. Conclusion and Future Work

This study proposed and validated a cost-effective, noninvasive hemoglobin monitoring device based on a single-wavelength near-infrared (NIR) LED (940 nm) and a photodiode sensor. The system demonstrated a strong correlation ($r = 0.9496$) between noninvasive and invasive hemoglobin values, with a normalized root mean squared error (NRMSE) of 0.6504 and a mean absolute percentage error (MAPE) of 0.0505. Classification using a k-nearest neighbor (kNN) algorithm achieved an overall accuracy of 90%, while Bland–Altman analysis confirmed a narrow agreement interval and minimal systematic bias. These findings establish the clinical relevance of the device for anemia and polycythemia screening, particularly in resource-limited or home-based settings. The simplicity of the hardware design, leveraging the optical window of biological tissue at 940 nm, and the use of a second-degree polynomial regression model for hemoglobin estimation further support the feasibility of real-time, noninvasive monitoring. Statistical validation and comparative analysis with existing systems demonstrate the proposed device's superior trade-off between accuracy, usability, and affordability.

Despite its promising performance, several avenues exist for improvement. Future research will focus on enhancing the system's robustness across varying skin pigmentation, finger size, and age groups by developing adaptive calibration algorithms. Additional work is needed to mitigate errors due to environmental contamination (e.g., dust, nail polish) and motion artifacts through signal filtering and real-time feedback mechanisms. Furthermore, expanding the system's capabilities to measure additional hemoglobin-related biomarkers—such as carboxyhemoglobin, methemoglobin, and glycated hemoglobin (HbA1c)—is a key future direction. Integration with mobile health platforms and cloud-based analytics may also enable longitudinal tracking and personalized diagnostics, making the device more versatile for clinical and telehealth applications. Large-scale clinical trials across diverse demographic populations will be necessary to generalize the findings and secure regulatory approval for widespread deployment.

Acknowledgment

The authors wish to thank Dept. of Biomedical Engineering staffs and all professor of this department for sporting equipment and other facilities. This work was not supported in part by a grant.

References

[1] Park, Y. H., Lim, S., Kang, H., Shin, H. Y., Baek, C. W., & Woo, Y. C. (2018). Comparison of the accuracy of noninvasive hemoglobin monitoring for preoperative evaluation between adult and pediatric patients: a retrospective study. Journal of Clinical Monitoring and Computing, 32(5). https://doi.org/10.1007/s10877-017-0098-8

[2] Jakacka, N., Snarski, E., & Mekuria, S. (2016). Prevention of iatrogenic anemia in critical and neonatal care. In Advances in Clinical and Experimental Medicine (Vol. 25, Issue 1). https://doi.org/10.17219/acem/32065

[3] Joseph, B., Pandit, V., Aziz, H., Kulvatunyou, N., Zangbar, B., Tang, A., O'Keeffe, T., Jehangir, Q., Snyder, K., & Rhee, P. (2015). Transforming hemoglobin measurement in trauma patients: Noninvasive spot check hemoglobin. Journal of the American College of Surgeons, 220(1). https://doi.org/10.1016/j.jamcollsurg.2014.09.022

[4] Hadar, E., Raban, O., Bouganim, T., Tenenbaum-Gavish, K., & Hod, M. (2012). Precision and accuracy of noninvasive hemoglobin measurements during pregnancy. Journal of Maternal-Fetal and Neonatal Medicine, 25(12). https://doi.org/10.3109/14767058.2012.704453

[5] Pinto, C., Parab, J., & Naik, G. (2020). Noninvasive hemoglobin measurement using embedded platform. Sensing and Bio-Sensing Research, 29. https://doi.org/10.1016/j.sbsr.2020.100370

[6] Elizabeth M. Staley, Joseph Schwartz, Huy P. Pham, Chapter 76 - Therapeutic Erythrocytapheresis and Red Cell Exchange, Editor(s): Beth H. Shaz, Christopher D. Hillyer, Morayma Reyes Gil, Transfusion Medicine and Hemostasis (Third Edition), Elsevier, 2019, Pages 477-479, ISBN 9780128137260, https://doi.org/10.1016/B978-0-12-813726-0.00076-3

[7] Chung, R. K., Wood, A. M., & Sweeting, M. J. (2019). Biases incurred from nonrandom repeat testing of haemoglobin levels in blood donors: Selective testing and its implications. Biometrical Journal, 61(2). https://doi.org/10.1002/bimj.201700268

[8] Halder, A., Sarkar, P. K., Pal, P., Chakrabarti, S., Chakrabarti, P., Bhattacharyya, D., Chakraborty, R., & Pal, S. K. (2017). Digital Camera-Based Spectrometry for the Development of Point-of-Care Anemia Detection on Ultra-Low Volume Whole Blood Sample. IEEE Sensors Journal, 17(21). https://doi.org/10.1109/JSEN.2017.2752371

[9] Garcá-Soler, P., Camacho Alonso, J. M., González-Gómez, J. M., & Milano-Manso, G. (2017). Noninvasive hemoglobin monitoring in critically ill pediatric patients at risk of bleeding. Medicina Intensiva (English Edition), 41(4). https://doi.org/10.1016/j.medine.2016.06.005

[10] Patel, A. J., Wesley, R., Leitman, S. F., & Bryant, B. J. (2013). Capillary versus venous haemoglobin determination in the assessment of healthy blood donors. *Vox Sanguinis*, *104*(4). https://doi.org/10.1111/vox.12006

[11] Gayat, E., Aulagnier, J., Matthieu, E., Boisson, M., & Fischler, M. (2012). Noninvasive measurement of hemoglobin: Assessment of two different point-of-care technologies. *PLoS ONE*, *7*(1). https://doi.org/10.1371/journal.pone.0030065

[12] Feng, X., Li, G., Yu, H., Wang, S., Yi, X., & Lin, L. (2018). Wavelength selection for portable noninvasive blood component measurement system based on spectral difference coefficient and dynamic spectrum. Spectrochimica Acta - Part A: Molecular and Biomolecular Spectroscopy, 193. https://doi.org/10.1016/j.saa.2017.10.063

[13] Joseph, B., Hadjizacharia, P., Aziz, H., Snyder, K., Wynne, J., Kulvatunyou, N., Tang, A., O'Keeffe, T., Latifi, R., Friese, R., & Rhee, P. (2013). Continuous noninvasive hemoglobin monitor from pulse Ox: Ready for prime time? World Journal of Surgery, 37(3). https://doi.org/10.1007/s00268-012-1871-y

[14] Sztefko, K., Beba, J., Mamica, K., & Tomasik, P. (2013). Blood loss from laboratory diagnostic tests in children. Clinical Chemistry and Laboratory Medicine, 51(8). https://doi.org/10.1515/cclm-2012-0672

[15] Slifer, K. J., Babbitt, R. L., & Cataldo, M. D. (1995). Simulation and Counterconditioning as Adjuncts to Pharmacotherapy for Invasive Pediatric Procedures. Journal of Developmental and Behavioral Pediatrics, 16(3). https://doi.org/10.1097/00004703-199506000-00001

[16] Slifer, K. J., Hankinson, J. C., Zettler, M. A., Frutchey, R. A., Hendricks, M. C., Ward, C. M., & Reesman, J. (2011). Distraction, exposure therapy, counterconditioning, and topical anesthetic for acute pain management during needle sticks in children with intellectual and developmental disabilities. Clinical Pediatrics, 50(8). https://doi.org/10.1177/0009922811398959

[17] Phillips, M. R., Khoury, A. L., Bortsov, A. v., Marzinsky, A., Short, K. A., Cairns, B. A., Charles, A. G., Joyner, B. L., & McLean, S. E. (2015). A noninvasive hemoglobin monitor in the pediatric intensive care unit. Journal of Surgical Research, 195(1). https://doi.org/10.1016/j.jss.2014.12.051

[18] Joseph B., Haider A., Rhee P.(2016). Noninvasive hemoglobin monitoring.International Journal of Surgery (2016), https://doi.org/10.1016/j.ijsu.2015.11.048

[19] Stassen, N. A., Bhullar, I., Cheng, J. D., Crandall, M. L., Friese, R. S., Guillamondegui, O. D., Jawa, R. S., Maung, A. A., Rohs, T. J., Sangosanya, A., Schuster, K. M., Seamon, M. J., Tchorz, K. M., Zarzuar, B. L., & Kerwin, A. J. (2012). Selective nonoperative management of blunt splenic injury: An eastern association for the surgery of trauma practice management guideline. In Journal of Trauma and Acute Care Surgery (Vol. 73, Issue 5 SUPPL.4). https://doi.org/10.1097/TA.0b013e3182702afc

[20] Dewhirst, E., Naguib, A., Winch, P., Rice, J., Galantowicz, M., McConnell, P., & Tobias, J. D. (2014). Accuracy of noninvasive and continuous hemoglobin measurement by pulse co-oximetry during preoperative phlebotomy. Journal of Intensive Care Medicine, 29(4). https://doi.org/10.1177/0885066613485355

[21] Wittenmeier, E., Bellosevich, S., Mauff, S., Schmidtmann, I., Eli, M., Pestel, G., & Noppens, R. R. (2015). Comparison of the gold standard of hemoglobin measurement with the clinical standard (BGA) and noninvasive hemoglobin measurement (SpHb) in small children: A prospective diagnostic observational study. Paediatric Anaesthesia, 25(10). https://doi.org/10.1111/pan.12683

[22] Timm, U., Lewis, E., McGrath, D., Kraitl, J., & Ewald, H. (2009). Sensor System Concept for Non-Invasive Blood Diagnosis. Procedia Chemistry, 1(1). https://doi.org/10.1016/j.proche.2009.07.123

[23] Pintavirooj, C., Ni, B., Chatkobkool, C., & Pinijkij, K. (2021). Noninvasive portable hemoglobin concentration monitoring system using optical sensor for anemia disease. *Healthcare (Switzerland)*, *9*(6). https://doi.org/10.3390/healthcare9060647

[24] Medicinenet.com, Hemoglobin: Normal, High, Low Levels and Causes, [Online]. Available: https://www.medicinenet.com/hemoglobin/article.htm

[25] JAMES H. GARVIN, 4 - Gender-Specific Aspects of Pediatric Hematology and Oncology, Editor(s): Marianne J. Legato, Principles of Gender-Specific Medicine, Academic Press, 2004, Pages 36-43, ISBN 9780124409057, https://doi.org/10.1016/B978-012440905-7/50268-1.
[26] Pintavirooj, C., Ni, B., Chatkobkool, C., & Pinijkij, K. (2021). Noninvasive portable hemoglobin concentration monitoring system using optical sensor for anemia disease. Healthcare (Switzerland), 9(6). https://doi.org/10.3390/healthcare9060647
[27] Hossain, S., Gupta, S. sen, Kwon, T. H., & Kim, K. D. (2021). Derivation and validation of gray-box models to estimate noninvasive in-vivo percentage glycated hemoglobin using digital volume pulse waveform. Scientific Reports, 11(1). https://doi.org/10.1038/s41598-021-91527-2
[28] Pintavirooj, C., Ni, B., Chatkobkool, C., & Pinijkij, K. (2021). Noninvasive portable hemoglobin concentration monitoring system using optical sensor for anemia disease. Healthcare (Switzerland), 9(6). https://doi.org/10.3390/healthcare9060647
[29] Maikala, R. v. (2010). Modified Beer's Law - historical perspectives and relevance in near-infrared monitoring of optical properties of human tissue. International Journal of Industrial Ergonomics, 40(2). https://doi.org/10.1016/j.ergon.2009.02.011
[30] Pascual-Gu àrdia, S., Ferrer, A., D áz, Ó., Caguana, A. O., Tejedor, E., Bellido-Calduch, S., Rodr íguez-Chiaradia, D. A., & Gea, J. (2021). Absence of Relevant Clinical Effects of SARS-COV-2 on the Affinity of Hemoglobin for O2 in Patients with COVID-19. Archivos de Bronconeumologia, 57(12). https://doi.org/10.1016/j.arbres.2021.03.015
[31] J. Kraitl, D. Klinger, D. Fricke, U. Timm, and H. Ewald, Noninvasive Measurement of Blood Components Sensors for an In-Vivo Haemoglobin Measurement. Springer-Verlag Berlin Heidelberg 2013.
[32] Patil, D. P. J., Thakare, D. G. V., & Patil, D. S. P. (2013). Variability And Accuracy Of Sahli's Method In Estimation Of Haemoglobin Concentration: Variability And Accuracy Of Sahli's Method In Estimation. National Journal of Integrated Research in Medicine, 4(1), 39-45. Retrieved from http://nicpd.ac.in/ojs-/index.php/njirm/article/view/2125
[33] Estimation of hemoglobin [Online]. Available: https://nios.ac.in/media/documents/dmlt/hbbt/Lesson-03.pdf
[34] Chanal, D., Yousfi Steiner, N., Petrone, R., Chamagne, D., & P éra, M.-C. (2021). Online Diagnosis of PEM Fuel Cell by Fuzzy C-Means Clustering. In Reference Module in Earth Systems and Environmental Sciences. https://doi.org/10.1016/b978-0-12-819723-3.00099-8
[35] Sarker, I. H. (2021). Machine Learning: Algorithms, Real-World Applications and Research Directions. SN Computer Science, 2(3). https://doi.org/10.1007/s42979-021-00592-x
[36] Sayilgan, E., Yüce, Y. K., & İŞler, Y. (2021). Evaluation of mother wavelets on steady-state visually-evoked potentials for triple-command brain-computer interfaces. Turkish Journal of Electrical Engineering and Computer Sciences, 25(9). https://doi.org/10.3906/elk-2010-26
[37] Doğan, N. Ö. (2018). Bland-Altman analysis: A paradigm to understand correlation and agreement. In Turkish Journal of Emergency Medicine (Vol. 18, Issue 4). https://doi.org/10.1016/j.tjem.2018.09.001
[38] Knutson, T., Della-Giustina, D., Tomich, E., Wills, B., Luerssen, E., & Reynolds, P. (2013). Evaluation of a new nonnvasive device in determining hemoglobin levels in emergency department patients. Western Journal of Emergency Medicine, 14(3). https://doi.org/10.5811/westjem.2011.9.6733
[39] Giavarina, D. (2015). Understanding Bland Altman analysis. Biochemia Medica, 25(2). https://doi.org/10.11613/BM.2015.015
[40] Passing, H., & Bablok, W. (2009). A New Biometrical Procedure for Testing the Equality of Measurements from Two Different Analytical Methods. Application of linear regression procedures for method comparison studies in Clinical Chemistry, Part I. Clinical Chemistry and Laboratory Medicine, 21(11). https://doi.org/10.1515/cclm.1983.21.11.709
[41] Sordillo, L. A., Pratavieira, S., Pu, Y., Salas-Ramirez, K., Shi, L., Zhang, L., Budansky, Y., & Alfano, R. R. (2014). Third therapeutic spectral window for deep tissue imaging. Optical Biopsy XII, 8940. https://doi.org/10.1117/12.2040604
[42] Pu, Y., Shi, L., Pratavieira, S., & Alfano, R. R. (2013). Two-photon excitation microscopy using the second singlet state of fluorescent agents within the "tissue optical window." Journal of Applied Physics, 114(15). https://doi.org/10.1063/1.4825319
[43] Rothman, L. S., Gordon, I. E., Babikov, Y., Barbe, A., Chris Benner, D., Bernath, P. F., Birk, M., Bizzocchi, L., Boudon, V., Brown, L. R., Campargue, A., Chance, K., Cohen, E. A., Coudert, L. H., Devi, V. M., Drouin, B. J., Fayt, A., Flaud, J. M., Gamache, R. R., … Wagner, G. (2013). The HITRAN2012 molecular spectroscopic database. Journal of Quantitative Spectroscopy and Radiative Transfer, 130. https://doi.org/10.1016/j.jqsrt.2013.07.002
[44] Kern, C. (2017). The difficulty of measuring the absorption of scattered sunlight by H2O and CO2 in volcanic plumes: A comment on pering et al. "A novel and inexpensive method for measuring volcanic plume water fluxes at high temporal resolution," Remote Sens. 2017, 9, 146. Remote Sensing, 9(6). https://doi.org/10.3390/rs9060534
[45] Kern, C. (2017). The difficulty of measuring the absorption of scattered sunlight by H2O and CO2 in volcanic plumes: A comment on pering et al. "A novel and inexpensive method for measuring volcanic plume water fluxes at high temporal resolution," Remote Sens. 2017, 9, 146. Remote Sensing, 9(6). https://doi.org/10.3390/rs9060534
[46] Kern, C., Masias, P., Apaza, F., Reath, K. A., & Platt, U. (2017). Remote measurement of high preeruptive water vapor emissions at Sabancaya volcano by passive differential optical absorption spectroscopy. Journal of Geophysical Research: Solid Earth, 122(5). https://doi.org/10.1002/2017JB014020
[47] Kavsaoılu, A. R., Polat, K., & Hariharan, M. (2015). Noninvasive prediction of hemoglobin level using machine learning techniques with the PPG signal's characteristics features. Applied Soft Computing Journal, 37. https://doi.org/10.1016/j.asoc.2015.04.008
[48] Nirupa, J. L. A., & Kumar, V. J. (2014). Noninvasive measurement of hemoglobin content in blood. IEEE MeMeA 2014 - IEEE International Symposium on Medical Measurements and Applications, Proceedings. https://doi.org/10.1109/MeMeA.2014.6860140
[49] Jeon, K. J., Kim, S.-J., Park, K. K., Kim, J.-W., & Yoon, G. (2002). Noninvasive total hemoglobin measurement. Journal of Biomedical Optics, 7(1). https://doi.org/10.1117/1.1427047
[50] Nguyen, B. V., Vincent, J. L., Nowak, E., Coat, M., Paleiron, N., Gouny, P., Ould-Ahmed, M., Guillouet, M., Arvieux, C. C., & Gueret, G. (2011). The accuracy of noninvasive hemoglobin measurement by multiwavelength pulse oximetry after cardiac surgery. Anesthesia and Analgesia, 113(5). https://doi.org/10.1213/ANE.0b013e31822c9679
[51] Yi, X., Li, G., & Lin, L. (2017). Noninvasive hemoglobin measurement using dynamic spectrum. Review of Scientific Instruments, 88(8). https://doi.org/10.1063/1.4998978

[52] Timm, U., Gewiss, H., Kraitl, J., Stuepmann, K., Hinz, M., Koball, S., & Ewald, H. (2015). Novel multi wavelength sensor concept to detect total hemoglobin concentration, methemoglobin and oxygen saturation. Optical Diagnostics and Sensing XV: Toward Point-of-Care Diagnostics, 9332. https://doi.org/10.1117/12.2080144

[53] Ding, H., Lu, Q., Gao, H., & Peng, Z. (2014). Noninvasive prediction of hemoglobin levels by principal component and back propagation artificial neural network. Biomedical Optics Express, 5(4). https://doi.org/10.1364/boe.5.001145

[54] Wang, E. J., Li, W., Zhu, J., Rana, R., & Patel, S. N. (2017). Noninvasive hemoglobin measurement using unmodified smartphone camera and white flash. Proceedings of the Annual International Conference of the IEEE Engineering in Medicine and Biology Society, EMBS. https://doi.org/10.1109/EMBC.2017.8037323

Authors' Profiles

Md. Altab Hossain received his B.Sc. degree in Biomedical Engineering from Khulna University of Engineering & Technology (KUET), Khulna, Bangladesh. His research interests include biomedical instrumentation, biomedical signal and image processing, machine learning in healthcare, clinical engineering, healthcare systems, and the study of brain function using functional near-infrared spectroscopy (fNIRS).

Dr. Sheikh Md. Rabiul Islam is a Professor in the Department of Electronics and Communication Engineering at Khulna University of Engineering & Technology (KUET), Bangladesh. He earned his Ph.D. in Information Sciences and Engineering from the University of Canberra, Australia, and holds master's degrees in both Telecommunication Engineering (University of Trento, Italy) and Public Health (ASA University, Bangladesh).

With over two decades of academic and research experience, Dr. Islam has authored more than 90 peer-reviewed journal articles and numerous international conference papers, focusing on biomedical signal processing, machine learning, antenna design, wireless communication, and FPGA-based systems. His recent works include cutting-edge research on EEG/fNIRS signal fusion, antenna optimization for 5G, and AI-driven diagnostics using medical imaging. He has received multiple research grants from the University Grants Commission (UGC), Bangladesh, and the Ministry of Science and Technology. He was honored with the Vice Chancellor's Research Award in both 2023 and 2024 for his outstanding scholarly output. Dr. Islam has supervised numerous postgraduate theses, including both M.Sc. and Ph.D. research, and serves as an external board member for other universities. He regularly contributes as a speaker at IEEE-sponsored international conferences and maintains a strong publication record in Scopus-indexed and Q1/Q2-ranked journals such as *MethodsX*, *Results in Engineering*, *Medical Reports*, and *Cognitive Neurodynamics*. He is affiliated with an IEEE Senior member. Further info on his homepage: www.kuet.ac.bd/ece/rabiul/.

How to cite this paper: Md. Altab Hossain, Sheikh Md. Rabiul Islam, "Noninvasive Hemoglobin Monitoring Device for Disease Detection", International Journal of Image, Graphics and Signal Processing(IJIGSP), Vol.17, No.6, pp. 60-76, 2025. DOI:10.5815/ijigsp.2025.06.04